A Learning-Based Approach for Traffic State Reconstruction from Limited Data

Nail Baloul, Amaury Hayat, Thibault Liard, Pierre Lissy[1]

PGMO Days, EDF Lab Paris-Saclay, Palaiseau

November, 19th 2025

[1]N. Baloul, A. Hayat, and P. Lissy are with CERMICS, ENPC and T. Liard is with XLIM, Université de Limoges

Table of Contents

Motivation

Traffic jam in Beijing

- Traffic congestion impacts urban *mobility* and *environmental* quality

Motivation

Traffic jam in Beijing

- Traffic management relies on **control** schemes to address perturbed traffic conditions
- Most existing control techniques require complete and accurate knowledge of state
- In practice, full information is rarely available due to limited and noisy measurements

Motivation

Traffic jam in Beijing

- **Goal** $\Rightarrow$ develop reliable methods for **estimating traffic from partial data**

Benchmark scales of traffic models

- microscopic $\Rightarrow$ individual vehicle dynamics, full information given

Microscopic model

- Simulation of agent-based dynamics
- Tracking position $x_i(t)$, velocity $v_i(t)$
- Each driver responds to surrounding traffic

$$\dot{v}_i(t) = F(v_i(t), x_i(t)) \tag{1}$$

[2] **francesco˙follow-leader˙2016**.

Traffic Flow Modeling Scales

Benchmark scales of traffic models

- macroscopic $\Rightarrow$ continuum representation using aggregated variables

Macroscopic model

- Traffic modelled as a continuous flow
- Density $\rho(t,x)$, speed $v(\rho)$, flux $f(\rho)$
- Total number of cars is conserved

$$0 = f(\rho(t,a)) - f(\rho(t,b)) = \frac{d}{dt}\int_a^b \rho(t,x)dx \tag{2}$$

[2] **francesco˙follow-leader˙2016**.

Traffic Flow Modeling Scales

Benchmark scales of traffic models

- microscopic ⇒ individual vehicle dynamics, full information given
- macroscopic ⇒ continuum representation using aggregated variables

Microscopic model

- Simulation of agent-based dynamics
- Tracking position $x_i(t)$, velocity $v_i(t)$
- Each driver responds to surrounding traffic

$$\dot{v}_i(t) = F(v_i(t), x_i(t)) \tag{1}$$

Macroscopic model

- Traffic modelled as a continuous flow
- Density $\rho(t,x)$, speed $v(\rho)$, flux $f(\rho)$
- Total number of cars is conserved

$$0 = f(\rho(t,a)) - f(\rho(t,b)) = \frac{d}{dt}\int_a^b \rho(t,x)dx \tag{2}$$

- **Connection** ⇒ macroscopic variables emerge from microscopic interactions[2]

---

[2] **francesco˙follow-leader˙2016**.

Microscopic Model

- 2 quantities *-only depending on time-* used to describe traffic systems
  $\Rightarrow$ state x_i *(position of vehicle* i *at time* t*)*
  $\Rightarrow$ velocity v_i *(speed of vehicle* i *at time* t*)*

Microscopic Model

- 2 quantities *-only depending on time-* used to describe traffic systems
  $\Rightarrow$ state x_i *(position of vehicle i at time t)*
  $\Rightarrow$ velocity v_i *(speed of vehicle i at time t)*
- Dynamics depend on **headway** $\Rightarrow$ captures reaction effects explicitly

$$\dot{x}_i(t) = v(z_i(t)) \tag{3}$$

where $z_i(t)$ accounts for *surrounding* of vehicle i

Macroscopic Model

- 3 quantities -*depending on space and time*- used to describe traffic systems
  $\Rightarrow$ relative density ρ *(number of vehicles per unit of length)*
  $\Rightarrow$ average velocity v *(mean speed of vehicles on a road segment)*
  $\Rightarrow$ flow rate f *(number of vehicles passing across a portion of the road during a period of time)*

Macroscopic Model

- 3 quantities *-depending on space and time-* used to describe traffic systems
  $\Rightarrow$ relative density ρ *(number of vehicles per unit of length)*
  $\Rightarrow$ average velocity v *(mean speed of vehicles on a road segment)*
  $\Rightarrow$ flow rate f *(number of vehicles passing across a portion of the road during a period of time)*
- **Fundamental diagram** of traffic flow $\Rightarrow$ $f(\rho) = \rho v_{\text{eq}}(\rho)$

Macroscopic Model

- 3 quantities *-depending on space and time-* used to describe traffic systems
  $\Rightarrow$ relative density ρ *(number of vehicles per unit of length)*
  $\Rightarrow$ average velocity v *(mean speed of vehicles on a road segment)*
  $\Rightarrow$ flow rate f *(number of vehicles passing across a portion of the road during a period of time)*
- **Fundamental diagram** of traffic flow $\Rightarrow f(\rho) = \rho v_{\text{eq}}(\rho)$
- **Hydrodynamic equation** and **conservation law** lead to LWR model

$$\frac{\partial}{\partial t}\rho + \frac{\partial}{\partial t}(\rho v_{\text{eq}}(\rho)) = 0 \tag{4}$$

where $v_{\text{eq}}(\rho)$ is the **equilibrium** velocity
$\Rightarrow$ vehicles immediately adjust their velocity to *match equilibrium*: $v(t,x) = v_{\text{eq}}(\rho)$
$\Rightarrow$ *neglects acceleration* effects and assumes traffic flow behaves as a compressible fluid

Table of Contents

Model-Based Approaches

- Follow-the-Leader (FtL), **microscopic** first order model
  $\Rightarrow$ dynamics of each vehicle depend on vehicle immediately in front

$$\begin{cases} \dot{x}_N^N(t) = v_{\max}, & t > 0, \\ \dot{x}_i^N(t) = v\left(\frac{L}{N(x_{i+1}^N(t) - x_i^N(t))}\right), & t > 0, \quad i = 0, \cdots, N-1 \\ x_i^N(0) = \bar{x}_i^N, & i = 0, \cdots, N \end{cases} \tag{5}$$

$\Rightarrow$ accurate traffic representation, encodes individual movements
$\Rightarrow$ computationally demanding, requires more data

- Lighthill-William-Richards (LWR), **macroscopic** traffic flow model
  $\Rightarrow$ vehicles treated as a continuous medium similar to particles in fluid
  $\Rightarrow$ one-dimensional (hyperbolic) conservation law

$$\begin{cases} \frac{\partial}{\partial t}\rho(t,x) + \frac{\partial}{\partial x} f(\rho(t,x)) = 0, & x \in \mathbb{R}, \quad t > 0, \\ \rho(0,x) = \bar{\rho}(x), & x \in \mathbb{R} \end{cases} \tag{6}$$

  $\Rightarrow$ faster implementation, less data-intensive
  $\Rightarrow$ overlooks traffic heterogeneity, oversimplifies traffic phenomena

- **Convergence analysis of FtL approximation scheme towards LWR model**[3]

[3] **holden˙continuum˙2017**.
[4] **francesco˙rigorous˙2015**.

- **Convergence analysis of FtL approximation scheme towards LWR model**[3]
- Link between FtL and LWR based on atomization of initial density $\bar{\rho}$

$$\bar{x}_{i+1}^N := \sup\left\{x \in \mathbb{R} : \int_{\bar{x}_i^N}^{x} \bar{\rho}(y)dy = \frac{L}{N}\right\}, \quad i = 0, \cdots, N-1 \tag{7}$$

[3] holden˙continuum˙2017.
[4] francesco˙rigorous˙2015.

Model-Based Approaches

- **Convergence analysis of FtL approximation scheme towards LWR model**[3]
- Link between FtL and LWR based on atomization of initial density $\bar{\rho}$

$$\bar{x}_{i+1}^N := \sup \left\{ x \in \mathbb{R} : \int_{\bar{x}_i^N}^{x} \bar{\rho}(y) dy = \frac{L}{N} \right\}, \quad i = 0, \cdots, N-1 \tag{7}$$

- Solution of PDE (5) can be recovered as many particle limit[4] of ODE system (6)

Model_scheme.pdf

Coupled Resolution of a Microscopic ODE System and a Macroscopic PDE

[3] **holden˙continuum˙2017**.
[4] **francesco˙rigorous˙2015**.

- Hybrid micro-macro models explored in traffic density reconstruction[5]

$$
\begin{cases}
\dot{x}_N^N(t) = v_{\max}, & t > 0, \\
\dot{x}_i^N(t) = v\left(\rho(t, x_i^N(t))\right), & t > 0, \quad i = 0, \cdots, N-1 \\
\dfrac{\partial}{\partial t}\rho(t,x) + \dfrac{\partial}{\partial x} f(\rho(t,x)) = \gamma^2 \dfrac{\partial^2}{\partial x^2}\rho(t,x), & x \in \mathbb{R}, \quad t > 0,
\end{cases} \tag{8}
$$

where $\gamma^2 \frac{\partial^2}{\partial x^2}$ *is a diffusion correction term to handle discontinuous solutions of original PDE*

[5] **barreau˙physics-informed˙2021**.
[6] **liu˙learning-based˙2020**.

- Hybrid micro-macro models explored in traffic density reconstruction[5]

$$\begin{cases} \dot{x}_N^N(t) = v_{\max}, & t > 0, \\ \dot{x}_i^N(t) = v\left(\rho(t, x_i^N(t))\right), & t > 0, \quad i = 0, \cdots, N-1 \\ \dfrac{\partial}{\partial t}\rho(t,x) + \dfrac{\partial}{\partial x} f(\rho(t,x)) = \gamma^2 \dfrac{\partial^2}{\partial x^2}\rho(t,x), & x \in \mathbb{R}, \quad t > 0, \end{cases} \tag{8}$$

where $\gamma^2 \frac{\partial^2}{\partial x^2}$ *is a diffusion correction term to handle discontinuous solutions of original PDE*

- **Partial state reconstruction**[6] using measurements from probe vehicles (PVs)
  $\Rightarrow$ low penetration rate $N_{\text{probes}} \ll N_{\text{total}}$
  $\Rightarrow$ recover density ρ from **limited** trajectories

[5] **barreau˙physics-informed˙2021**.
[6] **liu˙learning-based˙2020**.

- Hybrid micro-macro models explored in traffic density reconstruction[5]

$$\begin{cases} \dot{x}_N^N(t) = v_{\max}, & t > 0, \\ \dot{x}_i^N(t) = v\left(\rho(t, x_i^N(t))\right), & t > 0, \quad i = 0, \cdots, N-1 \\ \frac{\partial}{\partial t}\rho(t,x) + \frac{\partial}{\partial x} f(\rho(t,x)) = \gamma^2 \frac{\partial^2}{\partial x^2}\rho(t,x), & x \in \mathbb{R}, \quad t > 0, \end{cases} \tag{8}$$

where $\gamma^2 \frac{\partial^2}{\partial x^2}$ *is a diffusion correction term to handle discontinuous solutions of original PDE*

- **Partial state reconstruction**[6] using measurements from probe vehicles (PVs)
  $\Rightarrow$ low penetration rate $N_{\text{probes}} \ll N_{\text{total}}$
  $\Rightarrow$ recover density ρ from **limited** trajectories
- Requires access to real-time positions, densities and instantaneous speeds of PVs

[5] **barreau˙physics-informed˙2021**.
[6] **liu˙learning-based˙2020**.

Data-Driven Approaches

- **Prior approaches rely on knowledge of initial density** $\bar{\rho}$
  $\Rightarrow$ No access to this critical information, need to leverage available data

[5] **barreau˙physics-informed˙2021**.
[6] **liu˙learning-based˙2020**.

Table of Contents

Parametrized Microscopic Model

- **Limited data scenario** $\Rightarrow$ only **initial and final** $\left\{\left(\bar{x}_i^N, \bar{y}_i^N\right)\right\}_{i=0}^n$ positions of **PVs**

Parametrized Microscopic Model

- **Limited data scenario** $\Rightarrow$ only **initial and final** $\left\{\left(\bar{x}_i^N, \bar{y}_i^N\right)\right\}_{i=0}^{n}$ positions of **PVs**
- **Enhanced** version of FtL scheme (5) adding a parameter
  $\Rightarrow$ α^N accounts for unobserved vehicles between consecutive PVs
  $\Rightarrow$ bridges discrete (vehicle-level) dynamics to continuous (density-level) dynamics

Parametrized Microscopic Model

- **Limited data scenario** $\Rightarrow$ only **initial and final** $\left\{\left(\bar{x}_i^N, \bar{y}_i^N\right)\right\}_{i=0}^n$ positions of **PVs**
- **Enhanced** version of FtL scheme (5) adding a parameter
  $\Rightarrow$ α^N accounts for unobserved vehicles between consecutive PVs
  $\Rightarrow$ bridges discrete (vehicle-level) dynamics to continuous (density-level) dynamics
- Parametrized ODE system with **finite time horizon**

$$\begin{cases} \dot{x}_n^N(t) = v_{\max}, & t \in (0, T] \\ \dot{x}_i^N(t) = v\left(\rho_i^N(t)\right), & t \in (0, T] \quad i = 0, \cdots, n-1 \\ x_i^N(0) = \bar{x}_i^N, & i = 0, \cdots, n \end{cases} \tag{9}$$

$\Rightarrow$ local discrete densities

$$\rho_i^N(t) := \frac{\alpha_i^N L}{N\left(x_{i+1}^N(t) - x_i^N(t)\right)}, \quad t \in (0, T], \quad i = 0, \cdots, n-1 \tag{10}$$

Parametrized Microscopic Model

- **Limited data scenario** $\Rightarrow$ only **initial and final** $\left\{\left(\bar{x}_i^N, \bar{y}_i^N\right)\right\}_{i=0}^n$ positions of **PVs**
- **Enhanced** version of FtL scheme (5) adding a parameter
  $\Rightarrow$ α^N accounts for unobserved vehicles between consecutive PVs
  $\Rightarrow$ bridges discrete (vehicle-level) dynamics to continuous (density-level) dynamics
- Parametrized ODE system with **finite time horizon**

$$\begin{cases} \dot{x}_n^N(t) = v_{\max}, & t \in (0,T] \\ \dot{x}_i^N(t) = v\left(\rho_i^N(t)\right), & t \in (0,T] \quad i = 0, \cdots, n-1 \\ x_i^N(0) = \bar{x}_i^N, & i = 0, \cdots, n \end{cases} \tag{9}$$

$\Rightarrow$ local discrete densities

$$\rho_i^N(t) := \frac{\alpha_i^N L}{N\left(x_{i+1}^N(t) - x_i^N(t)\right)}, \quad t \in (0,T], \quad i = 0, \cdots, n-1 \tag{10}$$

- Piecewise constant Eulerian discrete density

$$\rho^N(t,x) := \sum_{i=0}^{N-1} \rho_i^N(t) \chi_{[x_i^N(t), x_{i+1}^N(t))}(x), \quad x \in \mathbb{R}, \quad t \in [0,T] \tag{11}$$

Well Posedness

- Assumptions on velocity

$$v \in C^1([0, +\infty)) \tag{12a}$$

$$v \text{ is decreasing on } [0, +\infty) \tag{12b}$$

$$v(0) = v_{\max} < \infty \tag{12c}$$

Well Posedness

- Assumptions on velocity

$$v \in C^1([0, +\infty)) \tag{12a}$$

$$v \text{ is decreasing on } [0, +\infty) \tag{12b}$$

$$v(0) = v_{\text{max}} < \infty \tag{12c}$$

- Local existence and uniqueness of solution to (9) (for fixed α) via Picard-Lindelöf

- Assumptions on velocity

$$v \in C^1([0,+\infty)) \tag{12a}$$
$$v \text{ is decreasing on } [0,+\infty) \tag{12b}$$
$$v(0) = v_{\max} < \infty \tag{12c}$$

- Local existence and uniqueness of solution to (9) (for fixed α) via Picard-Lindelöf
- Condition on initial car positions $\bar{x}_0^N < \bar{x}_1^N < \cdots < \bar{x}_{n-1}^N < \bar{x}_n^N$
  $\Rightarrow$ global existence

Lemma (Discrete maximum principle)

For solution $x(t)$ of (9) with v satisfying (12a)-(12c), for all $i = 0, \cdots, n-1$,

$$\frac{\alpha_i^N L}{NM} \leq x_{i+1}^N(t) - x_i^N(t) \leq \bar{x}_n^N - \bar{x}_0^N + (v_{\max} - v(M))\, t, \quad \forall t \in [0,T], \tag{13}$$

where $M := \max_i \left(\frac{\alpha_i^N L}{N(\bar{x}_{i+1}^N - \bar{x}_i^N)} \right)$

- Physical conditions on $\alpha := \alpha^N$ induce feasible set

$$\mathcal{A}^N := \left\{ \alpha \in \mathbb{R}^n : \quad \alpha_i \in \left[1, \bar{z}_i^N\right], \quad i = 0, \ldots, n-1, \quad \sum_{i=0}^{n-1} \alpha_i = N \right\} \tag{14}$$

with $\bar{z}_i^N := \min \left\{ \frac{N\left(\bar{x}_{i+1}^N - \bar{x}_i^N\right)}{L}, \frac{N\left(\bar{y}_{i+1}^N - \bar{y}_i^N\right)}{L} \right\}, \quad i = 0, \ldots, n-1$

[7] **baloul˙reconstruction˙2025**.

- Physical conditions on $\alpha := \alpha^N$ induce feasible set

$$\mathcal{A}^N := \left\{ \alpha \in \mathbb{R}^n : \quad \alpha_i \in \left[1, \bar{z}_i^N\right], \quad i = 0, \ldots, n-1, \quad \sum_{i=0}^{n-1} \alpha_i = N \right\} \tag{14}$$

with $\bar{z}_i^N := \min \left\{ \frac{N\left(\bar{x}_{i+1}^N - \bar{x}_i^N\right)}{L}, \frac{N\left(\bar{y}_{i+1}^N - \bar{y}_i^N\right)}{L} \right\}, \quad i = 0, \ldots, n-1$

- **Approximate density reconstruction**[7] $\Rightarrow$ find optimal interaction parameter α

$$\begin{aligned} \underset{\alpha}{\text{minimize}} \quad & \frac{1}{2} \|x(T) - \bar{y}\|^2 \\ \text{s.t.} \quad & \dot{x}(t) = V\left(W_\alpha x(t) + b_\alpha(t)\right) \\ & x(0) = \bar{x} \\ & \alpha \in \mathcal{A}^N \end{aligned} \tag{15}$$

[7] **baloul˙reconstruction˙2025**.

- Physical conditions on $\alpha := \alpha^N$ induce feasible set

$$\mathcal{A}^N := \left\{ \alpha \in \mathbb{R}^n : \quad \alpha_i \in \left[1, \bar{z}_i^N\right], \quad i = 0, \ldots, n-1, \quad \sum_{i=0}^{n-1} \alpha_i = N \right\} \tag{14}$$

with $\bar{z}_i^N := \min\left\{ \frac{N\left(\bar{x}_{i+1}^N - \bar{x}_i^N\right)}{L}, \frac{N\left(\bar{y}_{i+1}^N - \bar{y}_i^N\right)}{L} \right\}, \quad i = 0, \ldots, n-1$

- **Approximate density reconstruction**[7] $\Rightarrow$ find optimal interaction parameter α

$$\begin{aligned} & \underset{\alpha}{\text{minimize}} && \frac{1}{2}\left\|x(T) - \bar{y}\right\|^2 \\ & \text{s.t.} && \dot{x}(t) = V\left(W_\alpha x(t) + b_\alpha(t)\right) \\ &&& x(0) = \bar{x} \\ &&& \alpha \in \mathcal{A}^N \end{aligned} \tag{15}$$

- Existence of solutions guaranteed by continuity of $V := v \circ \frac{1}{\cdot}$ and compactness of $\mathcal{A}^N$

[7] baloul˙reconstruction˙2025.

ODE-Constrained Optimization

- Physical conditions on $\alpha := \alpha^N$ induce feasible set

$$\mathcal{A}^N := \left\{ \alpha \in \mathbb{R}^n : \quad \alpha_i \in \left[1, \bar{z}_i^N\right], \quad i = 0, \dots, n-1, \quad \sum_{i=0}^{n-1} \alpha_i = N \right\} \tag{14}$$

with $\bar{z}_i^N := \min\left\{ \frac{N\left(\bar{x}_{i+1}^N - \bar{x}_i^N\right)}{L}, \frac{N\left(\bar{y}_{i+1}^N - \bar{y}_i^N\right)}{L} \right\}, \quad i = 0, \dots, n-1$

- **Approximate density reconstruction**[7] $\Rightarrow$ find optimal interaction parameter α

$$\begin{aligned} \underset{\alpha}{\text{minimize}} \quad & \frac{1}{2} \left\| x(T) - \bar{y} \right\|^2 \\ \text{s.t.} \quad & \dot{x}(t) = V\left(W_\alpha x(t) + b_\alpha(t)\right) \\ & x(0) = \bar{x} \\ & \alpha \in \mathcal{A}^N \end{aligned} \tag{15}$$

- Existence of solutions guaranteed by continuity of $V := v \circ \frac{1}{\cdot}$ and compactness of $\mathcal{A}^N$
- No uniqueness (a priori) since nonlinear dynamics can lead to multiple minima

[7] **baloul˙reconstruction˙2025**.

Learning Method

- Dataset consists of **artificial data** based on simulated (classical) FtL dynamics (5)
- Sampling of PVs yielding a **balanced representation** of overall traffic

Learning Method

- Dataset consists of **artificial data** based on simulated (classical) FtL dynamics (5)
- Sampling of PVs yielding a **balanced representation** of overall traffic
- **Neural network** architecture designed to **understand dynamics of traffic**

Learning Method

- Dataset consists of **artificial data** based on simulated (classical) FtL dynamics (5)
- Sampling of PVs yielding a **balanced representation** of overall traffic
- **Neural network** architecture designed to **understand dynamics of traffic**
- Residual network (ResNet) where each block corresponds to a single time step
- Input $\bar{x}$ and state $x(.)$ is propagated by mirroring Euler discretization

$$x(t+\Delta t) = x(t) + V(Wx(t)+b)\Delta t \tag{16}$$

- Weights and biases W, b are functions of α

$$\begin{cases} W_{i,i} := -\frac{N}{\alpha_i L}, & i = 0, \dots, n-1, \\ W_{i,i+1} := \frac{N}{\alpha_i L}, & i = 1, \dots, n-2, \\ W_{i,j} := 0, & \text{otherwise}, \end{cases} \quad b_i(t) =:= \delta_{i,n} \frac{N}{\alpha_i L}\left(v_{\max} t + \bar{x}_n^N\right), \quad t \in [0, T] \tag{17}$$

- Nonlinear dynamic map V acts as physics grounded activation function
- Backpropagation to minimize predictions errors $\mathcal{L}^{\text{train}}(x(T), \bar{y}) = \frac{1}{n}\sum_{j=0}^{n} |x_j^{\alpha}(T) - \bar{y}_j^N|^2$

Neural Network for Constrained Optimization

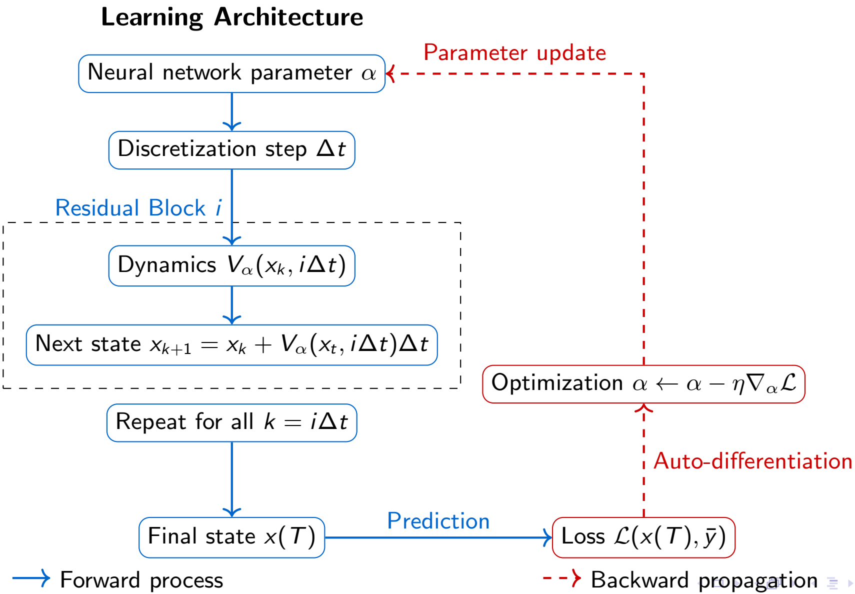

Model validation

- Through predicted parameter $\bar{\alpha}$, training yields piecewise constant discrete density

$$\rho^N(t,x) = \sum_{i=0}^{n-1} \frac{\bar{\alpha}_i L}{N(x_{i+1}^N(t) - x_i^N(t))} \chi_{[x_i^N(t), x_{i+1}^N(t))}(x), \quad x \in \mathbb{R}, \quad t \in [0, T], \tag{18}$$

Model validation

- Through predicted parameter $\bar{\alpha}$, training yields piecewise constant discrete density

$$\rho^N(t,x) = \sum_{i=0}^{n-1} \frac{\bar{\alpha}_i L}{N(x_{i+1}^N(t) - x_i^N(t))} \chi_{[x_i^N(t), x_{i+1}^N(t))}(x), \quad x \in \mathbb{R}, \quad t \in [0, T], \tag{18}$$

- Simulation on **test data** by solving ODE system

$$\begin{cases} \dot{x}_i^N(t) = v\left(\rho^N(t, x_i(t)^+)\right), & t \in (0, T], \\ x_i^N(0) = \bar{x}_i^N & i = 0, \dots, n_{\text{test}} \end{cases} \tag{19}$$

Model validation

- Through predicted parameter $\bar{\alpha}$, training yields piecewise constant discrete density

$$\rho^N(t,x) = \sum_{i=0}^{n-1} \frac{\bar{\alpha}_i L}{N(x_{i+1}^N(t) - x_i^N(t))} \chi_{[x_i^N(t), x_{i+1}^N(t))}(x), \quad x \in \mathbb{R}, \quad t \in [0,T], \tag{18}$$

- Simulation on **test data** by solving ODE system

$$\begin{cases} \dot{x}_i^N(t) = v\left(\rho^N(t, x_i(t)^+)\right), & t \in (0,T], \\ x_i^N(0) = \bar{x}_i^N & i = 0, \dots, n_{\text{test}} \end{cases} \tag{19}$$

- Assess model's performance by measuring test error $L^{\text{test}}(x(T), \bar{y}) = \dfrac{1}{n_{\text{test}}} \displaystyle\sum_{j=0}^{n_{\text{test}}} |x_j^{\bar{\alpha}}(T) - \bar{y}_i^N|^2$

Theorem Convergence of approximate density to solution of LWR

Under some assumptions, piecewise-constant density

$$\rho^N(t,x) = \sum_{i=0}^{n-1} \frac{\bar{\alpha}_i^N L}{N(x_{i+1}^N(t) - x_i^N(t))} \chi_{[x_i^N(t), x_{i+1}^N(t))}(x), \quad x \in \mathbb{R}, \quad t \in [0, T], \tag{21}$$

where $\bar{\alpha}_i^N \in \mathcal{A}^N$ is a solution to (15) converges to **unique entropy** solution ρ of

$$\begin{cases} \dfrac{\partial}{\partial t}\rho(t,x) + \dfrac{\partial}{\partial x} f(\rho(t,x)) = 0, \quad x \in \mathbb{R}, \quad t \in [0, T], \\ \rho(0,x) = \bar{\rho}(x), \quad x \in \mathbb{R} \end{cases} \tag{22}$$

Convergence Result

- Weak solution of (6) is entropy admissible if it satisfies **Kruzhkov entropy condition**

$$\int_0^T \int_{\mathbb{R}} |u-k| \frac{\partial \phi}{\partial t} + \text{sign}(u-k)(f(u)-f(k)) \frac{\partial \phi}{\partial x} dxdt \geq 0, \quad \forall k \in \mathbb{R} \tag{20}$$

Theorem Convergence of approximate density to solution of LWR

Under some assumptions, piecewise-constant density

$$\rho^N(t,x) = \sum_{i=0}^{n-1} \frac{\bar{\alpha}_i^N L}{N(x_{i+1}^N(t) - x_i^N(t))} \chi_{[x_i^N(t), x_{i+1}^N(t))}(x), \quad x \in \mathbb{R}, \quad t \in [0,T], \tag{21}$$

where $\bar{\alpha}_i^N \in \mathcal{A}^N$ is a solution to (15) converges to **unique entropy** solution ρ of

$$\begin{cases} \frac{\partial}{\partial t}\rho(t,x) + \frac{\partial}{\partial x} f(\rho(t,x)) = 0, \quad x \in \mathbb{R}, \quad t \in [0,T], \\ \rho(0,x) = \bar{\rho}(x), \quad x \in \mathbb{R} \end{cases} \tag{22}$$

- Impose a condition that ensures controlled growth of α^N

Scheme of Model

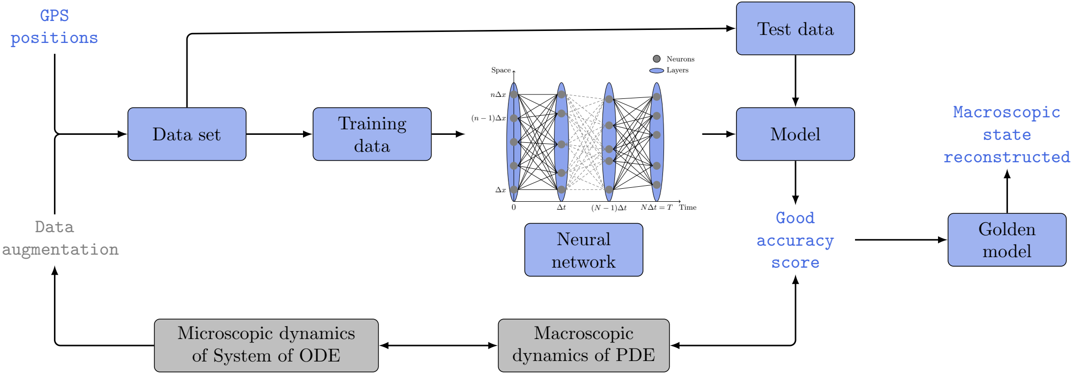

Traffic Flow Reconstruction Pipeline

Table of Contents

Numerical experiments

- Parameters
  - Maximum traffic speed $v_{\max} = 120$ km/h
  - Maximum traffic density $\rho_{\max} = 200$ cars/km
  - Greenshields velocity $v(\rho) = v_{\max} \max\left\{1 - \frac{\rho}{\rho_{max}}, 0\right\}, \quad \rho \in [0, \rho_{max}]$
  - Final time horizon $T = 0.1$ h or $T = 0.2$
- Sampling such 10% **of total fleet serve as PVs for training and** 2.5% **for testing**

Numerical experiments

- Parameters
  - Maximum traffic speed $v_{\text{max}} = 120$ km/h
  - Maximum traffic density $\rho_{\text{max}} = 200$ cars/km
  - Greenshields velocity $v(\rho) = v_{\text{max}} \max\left\{1 - \frac{\rho}{\rho_{max}}, 0\right\}, \quad \rho \in [0, \rho_{max}]$
  - Final time horizon $T = 0.1$ h or $T = 0.2$
- Sampling such 10% **of total fleet serve as PVs for training and** 2.5% **for testing**
- Three traffic scenarii modelled
  1. Rarefaction wave represents a smooth transition in traffic conditions
  2. Shock wave represents an abrupt transition in traffic conditions
  3. Stop-and-go wave characterized by alternating regions of congestion and free flow

Rarefaction wave scenario

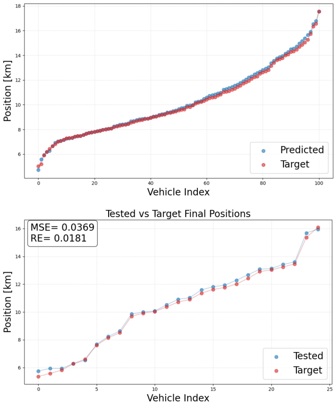

(a) $N = 1000$

Comparison of predicted and target final PV positions: **Top** Results from **training** procedure, **Bottom** Results on **test** sounds

Rarefaction wave scenario

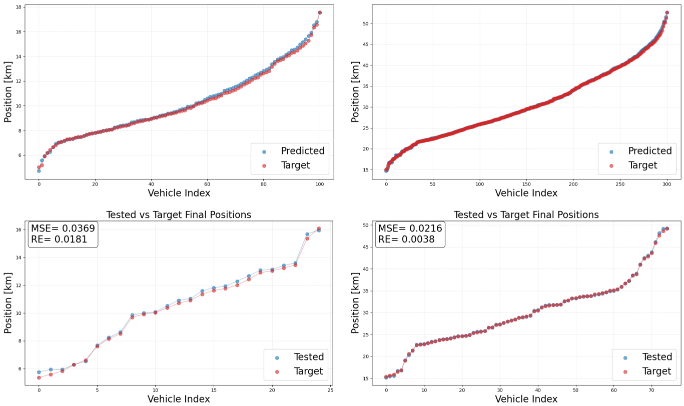

(a) $N = 1000$ (b) $N = 3000$

Comparison of predicted and target final PV positions: **Top** Results from **training** procedure, **Bottom** Results on **test** sounds

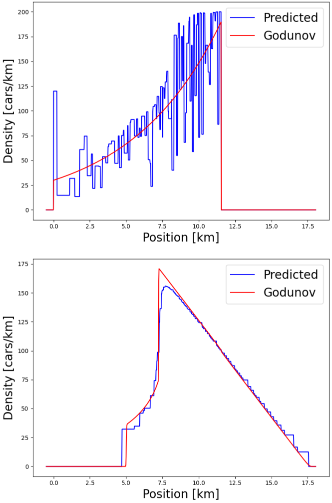

(a) $N = 1000$

Comparison of reconstructed and macroscopic densities: **Top** Initial densities, **Bottom** Final densities

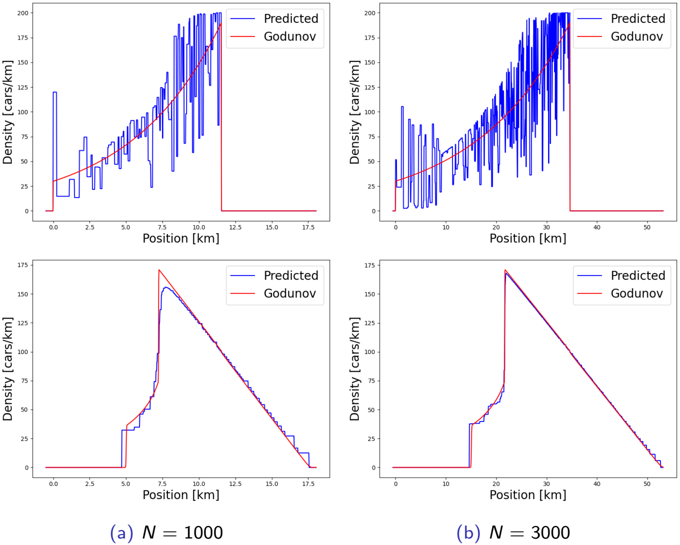

Comparison of reconstructed and macroscopic densities: **Top** Initial densities, **Bottom** Final densities

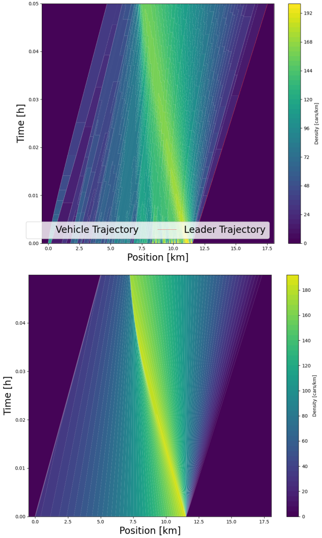

(a) $N = 1000$

Comparison of **reconstructed** and **macroscopic** densities: **Top** Reconstructed density, **Bottom** Godunov LWR density

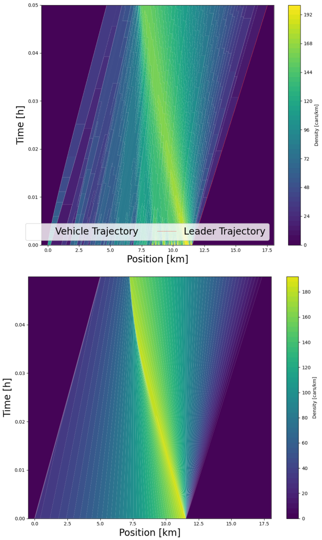

(a) $N = 1000$

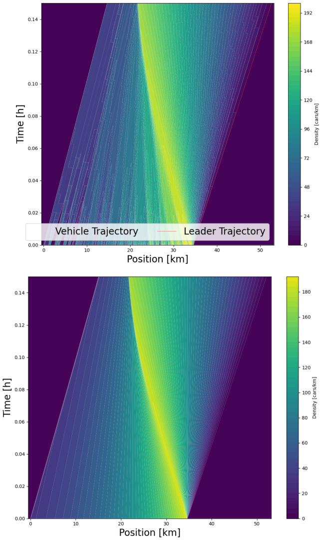

(b) $N = 3000$

Comparison of **reconstructed** and **macroscopic** densities: **Top** Reconstructed density, **Bottom** Godunov LWR density

Shock wave scenario

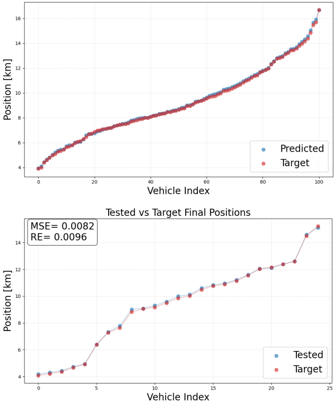

(a) $N = 1000$

Comparison of predicted and target final PV positions: **Top** Results from **training** procedure, **Bottom** Results on **test** sounds

Shock wave scenario

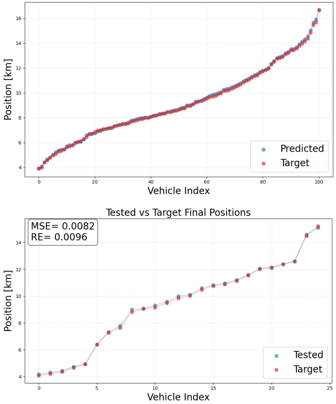

(a) $N = 1000$

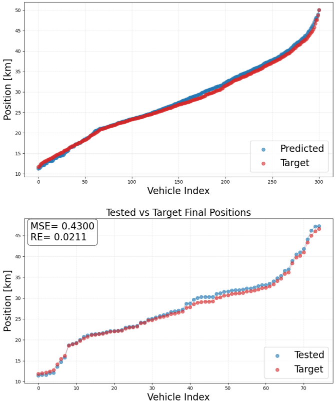

(b) $N = 3000$

Comparison of predicted and target final PV positions: **Top** Results from **training** procedure, **Bottom** Results on **test** sounds

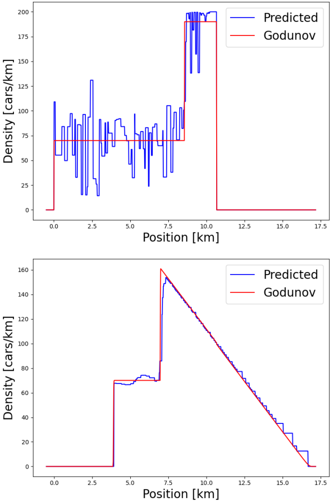

(a) $N = 1000$

Comparison of reconstructed and macroscopic densities: **Top** Initial densities, **Bottom** Final densities

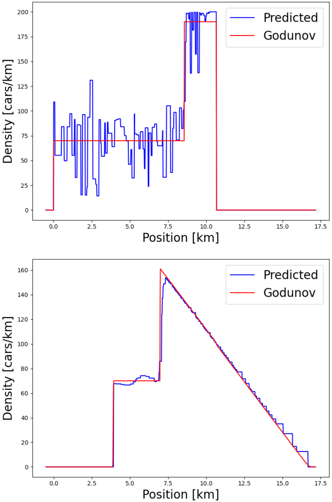

(a) $N = 1000$

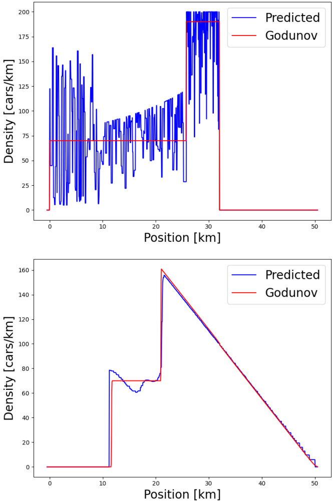

(b) $N = 3000$

Comparison of reconstructed and macroscopic densities: **Top** Initial densities, **Bottom** Final densities

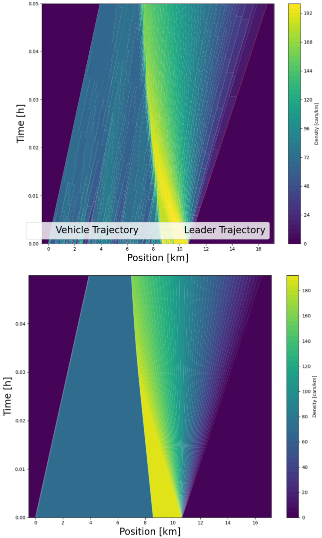

(a) $N = 1000$

Comparison of **reconstructed** and **macroscopic** densities: **Top** Reconstructed density, **Bottom** Godunov LWR density

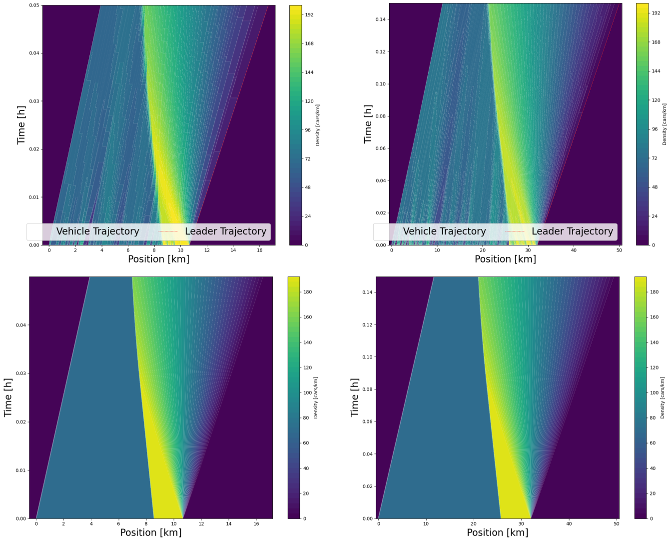

(a) $N = 1000$ (b) $N = 3000$

Comparison of **reconstructed** and **macroscopic** densities: **Top** Reconstructed density, **Bottom** Godunov LWR density

Stop-and-go wave scenario

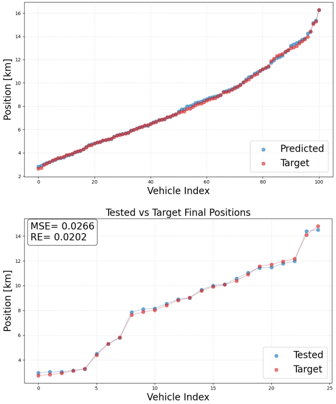

(a) $N = 1000$

Comparison of predicted and target final PV positions: **Top** Results from **training** procedure, **Bottom** Results on **test** sounds

Stop-and-go wave scenario

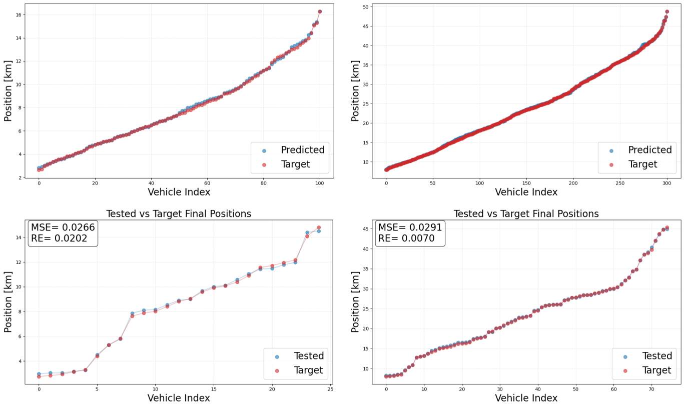

(a) $N = 1000$ (b) $N = 3000$

Comparison of predicted and target final PV positions: **Top** Results from **training** procedure, **Bottom** Results on **test** sounds

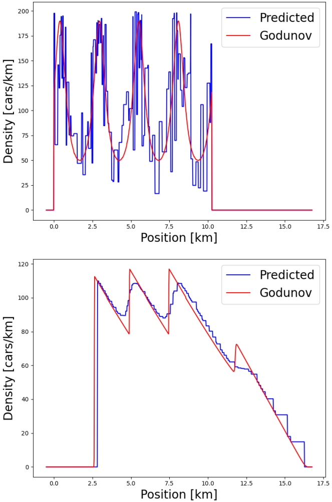

(a) $N = 1000$

Comparison of reconstructed and macroscopic densities: **Top** Initial densities, **Bottom** Final densities

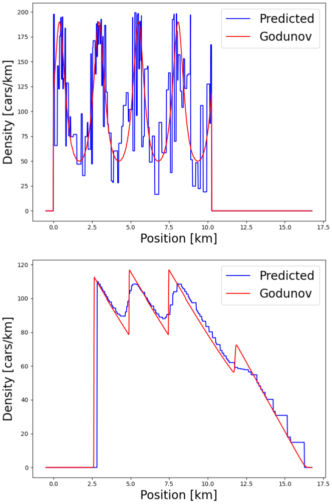

(a) $N = 1000$

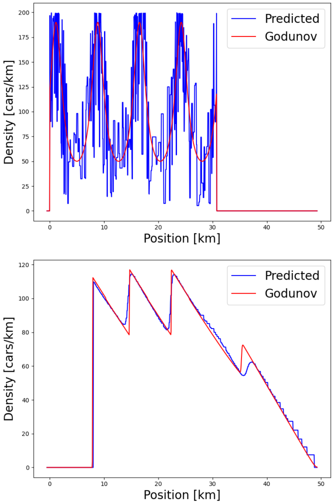

(b) $N = 3000$

Comparison of reconstructed and macroscopic densities: **Top** Initial densities, **Bottom** Final densities

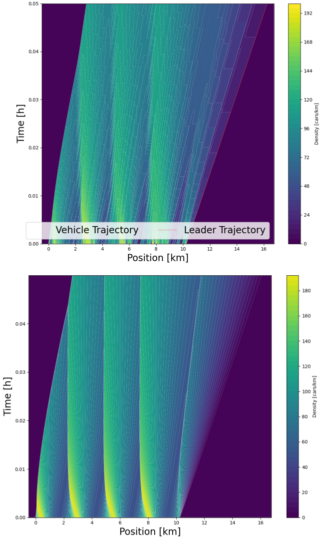

(a) $N = 1000$

Comparison of **reconstructed** and **macroscopic** densities: **Top** Reconstructed density, **Bottom** Godunov LWR density

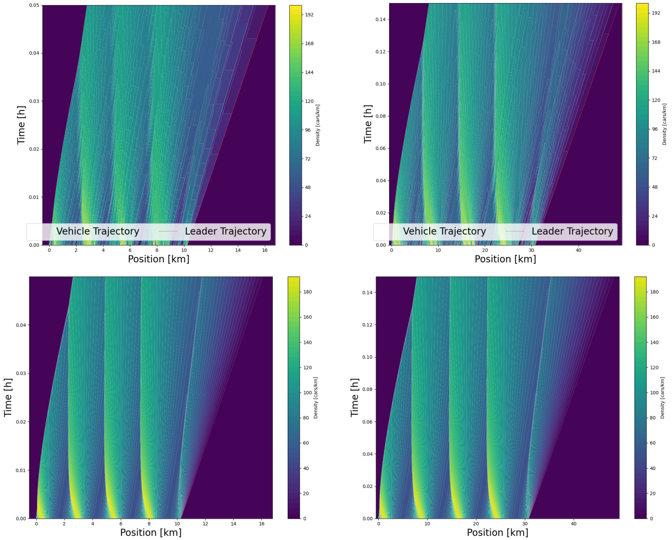

(a) $N = 1000$ (b) $N = 3000$

Comparison of **reconstructed** and **macroscopic** densities: **Top** Reconstructed density, **Bottom** Godunov LWR density

Table of Contents

Traffic State Reconstruction Approaches

- Model-Based Method
  $\Rightarrow$ uses microscopic and macroscopic models
  $\Rightarrow$ provides theoretical guarantees
  $\Rightarrow$ struggles to capture real-world complexities

Traffic State Reconstruction Approaches

- Model-Based Method
  - $\Rightarrow$ uses microscopic and macroscopic models
  - $\Rightarrow$ provides theoretical guarantees
  - $\Rightarrow$ struggles to capture real-world complexities
- Data-Driven Method
  - $\Rightarrow$ learns patterns directly from measurement data
  - $\Rightarrow$ derives system properties or predicts near-future states
  - $\Rightarrow$ requires extensive data for effectiveness

Traffic State Reconstruction Approaches

- Model-Based Method
  - ⇒ uses microscopic and macroscopic models
  - ⇒ provides theoretical guarantees
  - ⇒ struggles to capture real-world complexities
- Data-Driven Method
  - ⇒ learns patterns directly from measurement data
  - ⇒ derives system properties or predicts near-future states
  - ⇒ requires extensive data for effectiveness
- Our Approach
  - ⇒ combines models and data to address sparsity and improve realism
  - ⇒ **Integrates physical priors with data observations**
  - ⇒ achieves reliable traffic reconstruction with limited observations

- Conservation law with unilateral constraint[8] (toll gate)

$$\begin{cases} \dfrac{\partial}{\partial t}\rho(t,x) + \dfrac{\partial}{\partial x} f(\rho(t,x)) = 0, & x \in \mathbb{R}, \quad t > 0, \\ \rho(0,x) = \bar{\rho}(x), & x \in \mathbb{R}, \\ f(\rho(t,0)) \leq q(t), & t > 0. \end{cases} \tag{23}$$

[8] **colombo˙well˙2007**.
[9] **liard˙entropic˙2020**.

Perspectives

- Conservation law with unilateral constraint[8] (toll gate)

$$\begin{cases} \dfrac{\partial}{\partial t}\rho(t,x) + \dfrac{\partial}{\partial x} f(\rho(t,x)) = 0, & x \in \mathbb{R}, \quad t > 0, \\ \rho(0,x) = \bar{\rho}(x), & x \in \mathbb{R}, \\ f(\rho(t,0)) \leq q(t), & t > 0. \end{cases} \tag{23}$$

- Conservation law with moving bottleneck[9] (slow vehicle)

$$\begin{cases} \dfrac{\partial}{\partial t}\rho(t,x) + \dfrac{\partial}{\partial x} f(\rho(t,x)) = 0, & x \in \mathbb{R}, \quad t > 0, \\ \rho(0,x) = \bar{\rho}(x), & x \in \mathbb{R}, \\ f\left(\rho(t,y(t))\right) - \dot{y}(t)\rho(t,y(t)) \leq \frac{\alpha \rho_{\max}}{4 v_{\max}} \left(v_{\max} - \dot{y}(t)\right)^2, & t > 0, \\ \dot{y}(t) = \omega\left(\rho(t,y(t)_+)\right), & t > 0, \\ y(0) = y_0 \end{cases} \tag{24}$$

[8] colombo˙well˙2007.
[9] liard˙entropic˙2020.

- Network[10] with a junction[11] J and N incoming roads and M outgoing ones

$$\begin{cases} \frac{\partial}{\partial t}\rho_l(t,x) + \frac{\partial}{\partial x}\left(f(\rho_l(t,x))\right) = 0, & t > 0, \quad x \in I_l, \quad l = 1,\dots,N+M \\ \rho_l(0,x) = \rho_{0,l}(x), & x \in I_l = [a_l, b_l], \quad l = 1,\dots,N+M \end{cases} \tag{25}$$

$$\Rightarrow \sum_{i=1}^{N} f\left(\rho_i(t,(b_i)_-)\right) = \sum_{j=N+1}^{N+M} f\left(\rho_j(t,(a_j)_+)\right) \text{ (Rankine Hugoniot)}$$

$$\Rightarrow \sum_{i=1}^{N} f\left(\rho_i(t,(b_i)_-)\right) \text{ is maximized}^{12} \text{ s.t. } f\left(\rho_j(\cdot,(a_j)_+)\right) = \sum_{i=1}^{N} a_{j,i} f\left(\rho_i(\cdot,(b_i)_-)\right)$$

[10] monneau˙structure˙2024.
[11] coclite˙traffic˙2005.
[12] garavello2006traffic.

References I

Lemma (Discrete maximum principle)

For solution $x(t)$ of (9) with v satisfying (12a)-(12c), for all $i = 0, \cdots, n-1$,

$$\frac{\alpha_i^N L}{NM} \le x_{i+1}^N(t) - x_i^N(t) \le \bar{x}_n^N - \bar{x}_0^N + (v_{\max} - v(M))\, t, \quad \forall t \in [0, T], \tag{26}$$

where $M := \max_i \left(\frac{\alpha_i^N L}{N(\bar{x}_{i+1}^N - \bar{x}_i^N)} \right)$

Sketch of proof

- Lower bound is satisfied at $t = 0$, aim at extending property for all times up to T

Sketch of proof

- Lower bound is satisfied at $t = 0$, aim at extending property for all times up to T
- Equivalent to show

$$\inf_{0<t\leq T} [x_{i+1}(t) - x_i(t)] \geq \frac{\alpha_i^N L}{NM}, \quad i = 0, \ldots, n-1. \tag{27}$$

$\Rightarrow$ **recursive argument** (backward from $n-1$ to 0)

Sketch of proof

- Lower bound is satisfied at $t=0$, aim at extending property for all times up to T
- Equivalent to show

$$\inf_{0<t\leq T}[x_{i+1}(t)-x_i(t)]\geq\frac{\alpha_i^N L}{NM},\quad i=0,\dots,n-1. \tag{27}$$

$\Rightarrow$ **recursive argument** (backward from $n-1$ to 0)

- Property is true for $i=n-1$

$$\begin{aligned}x_n(t)-x_{n-1}(t)=&\bar{x}_n-\bar{x}_{n-1}+\int_0^t\left(v_{\max}-v\left(\frac{\alpha_n^N L}{N(x_n(s)-x_{n-1}(s))}\right)\right)ds\\ \geq&\bar{x}_n-\bar{x}_{n-1}\geq\frac{\alpha_{n-1}^N L}{NM}.\end{aligned}$$

Sketch of proof

- Lower bound is satisfied at $t = 0$, aim at extending property for all times up to T
- Equivalent to show

$$\inf_{0<t\leq T} [x_{i+1}(t) - x_i(t)] \geq \frac{\alpha_i^N L}{NM}, \quad i = 0, \ldots, n-1. \tag{27}$$

$\Rightarrow$ **recursive argument** (backward from $n-1$ to 0)

- Property is true for $i = n-1$

$$\begin{aligned} x_n(t) - x_{n-1}(t) =& \bar{x}_n - \bar{x}_{n-1} + \int_0^t \left(v_{\max} - v\left(\frac{\alpha_n^N L}{N(x_n(s) - x_{n-1}(s))} \right) \right) ds \\ \geq& \bar{x}_n - \bar{x}_{n-1} \geq \frac{\alpha_{n-1}^N L}{NM}. \end{aligned}$$

- Assume property is verified for $j+1$ and prove it is still satisfied for j

$$\inf_{0<t\leq T} [x_{j+2}(t) - x_{j+1}(t)] \geq \frac{\alpha_{j+1}^N L}{NM}. \tag{28}$$

Sketch of proof

- By contradiction, assume that there exists $0 \leq t_1 < t_2$ such that

$$
\begin{cases}
x_{j+1}(t) - x_j(t) \geq \frac{\alpha_j^N L}{NM}, & t < t_1 \\
x_{j+1}(t) - x_j(t) = \frac{\alpha_j^N L}{NM}, & t = t_1 \\
x_{j+1}(t) - x_j(t) < \frac{\alpha_j^N L}{NM}, & t_1 < t \leq t_2.
\end{cases}
\tag{29}
$$

Sketch of proof

- By contradiction, assume that there exists $0 \leq t_1 < t_2$ such that

$$\begin{cases} x_{j+1}(t) - x_j(t) \geq \frac{\alpha_j^N L}{NM}, & t < t_1 \\ x_{j+1}(t) - x_j(t) = \frac{\alpha_j^N L}{NM}, & t = t_1 \\ x_{j+1}(t) - x_j(t) < \frac{\alpha_j^N L}{NM}, & t_1 < t \leq t_2. \end{cases} \tag{29}$$

- Since v is decreasing

$$\begin{aligned} x_j(t) =& x_j(t_1) + \int_{t_1}^{t} v\left(\frac{\alpha_j^N L}{N(x_{j+1}(s) - x_j(s))}\right) ds \\ \leq& x_j(t_1) + v\left(M\right)\left(t - t_1\right), \end{aligned}$$

- Moreover from (28), for $t_1 < t \leq t_2$,

$$x_{j+1}(t) = x_{j+1}(t_1) + \int_{t_1}^{t} v\left(\frac{\alpha_{j+1}^N L}{N(x_{j+2}(s) - x_{j+1}(s))}\right) ds \geq x_{j+1}(t_1) + v\left(M\right)\left(t - t_1\right)$$

$$\Rightarrow x_{j+1}(t) - x_j(t) \geq x_{j+1}(t_1) - x_j(t_1) = \frac{\alpha_j^N L}{NM}$$

which contradicts (29), so that (27) is satisfied

Sketch of proof

- Show upper bound for $i = 0, \ldots, n-1$ and $t \in [0, T]$
- Recalling assumptions on v and applying system's dynamics

$$
\begin{aligned}
x_{i+1}(t) - x_i(t) &= x_{i+1}(0) - x_i(0) + \int_0^t \left(\dot{x}_{i+1}(s) - \dot{x}_i(s)\right) ds \\
&\leq \bar{x}_{i+1} - \bar{x}_i + \int_0^t \left(v_{\max} - v\left(\frac{\alpha_i^N L}{N(x_{i+1}(s) - x_i(s))} \right) \right) ds \\
&\leq \bar{x}_n - \bar{x}_0 + (v_{\max} - v(M))\, t,
\end{aligned}
$$

- Last equality is obtained from lower bound $\Rightarrow$ proof is complete

Outline of Convergence Analysis

- Prove that ρ^N predicted by ML converges to solution of LWR (6) when the $N \to \infty$

Outline of Convergence Analysis

- Prove that ρ^N predicted by ML converges to solution of LWR (6) when the $N \to \infty$
- Main challenge is imposing a condition on distribution of α which would guarantee convergence

Outline of Convergence Analysis

- Prove that ρ^N predicted by ML converges to solution of LWR (6) when the $N \to \infty$
- Main challenge is imposing a condition on distribution of α which would guarantee convergence
- Demonstrate that $\rho^N(0, \cdot)$ converges to $\bar{\rho}$ in LWR (6)

- Prove that ρ^N predicted by ML converges to solution of LWR (6) when the $N \to \infty$
- Main challenge is imposing a condition on distribution of α which would guarantee convergence
- Demonstrate that $\rho^N(0,\cdot)$ converges to $\bar{\rho}$ in LWR (6)
- Consider empirical discrete density

$$\widehat{\rho}^N(t,\cdot) := \frac{L}{N}\sum_{i=0}^{n-1} \alpha_i^N \delta_{x_i(t)}(\cdot), \quad t \in [0,T]. \tag{30}$$

Outline of Convergence Analysis

- Prove that ρ^N predicted by ML converges to solution of LWR (6) when the $N \to \infty$
- Main challenge is imposing a condition on distribution of α which would guarantee convergence
- Demonstrate that $\rho^N(0,\cdot)$ converges to $\bar{\rho}$ in LWR (6)
- Consider empirical discrete density

$$\widehat{\rho}^N(t,\cdot) := \frac{L}{N}\sum_{i=0}^{n-1} \alpha_i^N \delta_{x_i(t)}(\cdot), \quad t \in [0,T]. \tag{30}$$

- **Important observation**: by construction, initial traffic density must satisfy

$$\bar{x}_{i+1} = \sup\left\{x \in \mathbb{R} : \int_{\bar{x}_i}^{x} \bar{\rho}(y)dy \le \frac{\alpha_i L}{N}\right\}, \quad i = 0,\dots,n-1 \tag{31}$$

$\Rightarrow$ although no access to ground-truth initial car density $\bar{\rho}$, initial positions $\bar{x}_i$ verify (31)

Theorem Convergence of approximate density to solution of LWR

Under some assumptions, piecewise-constant density

$$\rho^N(t,x) = \sum_{i=0}^{n-1} \frac{\bar{\alpha}_i^N L}{N(x_{i+1}^N(t) - x_i^N(t))} \chi_{[x_i^N(t), x_{i+1}^N(t))}(x), \quad x \in \mathbb{R}, \quad t \in [0,T], \tag{32}$$

where $\bar{\alpha}_i^N \in \mathcal{A}^N$ is a solution to (15) converges to **unique entropy** solution ρ of

$$\begin{cases} \dfrac{\partial}{\partial t}\rho(t,x) + \dfrac{\partial}{\partial x} f(\rho(t,x)) = 0, \quad x \in \mathbb{R}, \quad t \in [0,T], \\ \rho(0,x) = \bar{\rho}(x), \quad x \in \mathbb{R} \end{cases} \tag{33}$$

Sketch of proof

- Ensures discretization aligns consistently with true initial density when $N \to \infty$
- Notations: for $t \in [0, T]$, $\rho(t) := \rho(t, \cdot)$ and $\widehat{\rho}(t) := \widehat{\rho}(t, \cdot)$
  In particular, at $t = 0$, $\rho(0) := \rho(0, \cdot)$ and $\widehat{\rho}(0) := \widehat{\rho}(0, \cdot)$

- Ensures discretization aligns consistently with true initial density when $N \to \infty$
- Notations: for $t \in [0, T]$, $\rho(t) := \rho(t, \cdot)$ and $\widehat{\rho}(t) := \widehat{\rho}(t, \cdot)$
  In particular, at $t = 0$, $\rho(0) := \rho(0, \cdot)$ and $\widehat{\rho}(0) := \widehat{\rho}(0, \cdot)$
- Use **Wasserstein distance** defined in **francesco˙rigorous˙2015** by

$$\mathrm{W}_{L,1}(f, g) = \|f(]-\infty, \cdot]) - g(]-\infty, \cdot]\|_{L^1(\mathbb{R},\mathbb{R})} \tag{34}$$

Proposition

Let $\bar{\rho}$ satisfy (31) and assume that

$$\max_{i=0,\dots,n-1} \alpha_i^N = o(N) \tag{35}$$

Then $(\rho^N(0))_{n\in\mathbb{N}}$ and $(\widehat{\rho}^N(0))_{n\in\mathbb{N}}$ converge to $\bar{\rho}$ in the sense of the $\mathrm{W}_{L,1}$ -Wasserstein distance in (34)

Remark

A particular case of assumption (35) is when $\max_{i=0,\dots,n-1} \alpha_i^N \leq \frac{CN}{\log(N)}$ for some $C > 0$

Sketch of proof

- Using $l_N := L/N$, $\mathrm{W}_{L,1}$- distance and discrete density in (10)

$$\begin{aligned} \mathrm{W}_{L,1}(\rho^N(0), \widehat{\rho}^N(0)) &= \sum_{i=0}^{n-1} \int_{\bar{x}_i}^{\bar{x}_{i+1}^N} \left(\alpha_i^N l_N - \rho_i^N(t)\,(x - \bar{x}_i) \right) dx \\ &= \sum_{i=0}^{n-1} \alpha_i^N l_N \int_{\bar{x}_i}^{\bar{x}_{i+1}} \left(1 - \frac{x - \bar{x}_i}{\bar{x}_{i+1} - \bar{x}_i} \right) dx \\ &\leq \max_{i=0,\dots,n} \{\alpha_i^N\} l_N \,(\bar{x}_n - \bar{x}_0) \end{aligned} \tag{36}$$

$\Rightarrow$ it suffices to prove that $(\widehat{\rho}^N(0))_{n\in\mathbb{N}}$ converges to $\bar{\rho}$ in sense of $\mathrm{W}_{L,1}$- distance

Sketch of proof

- Using $l_N := L/N$, $\mathrm{W}_{L,1}$- distance and discrete density in (10)

$$\begin{aligned}
\mathrm{W}_{L,1}(\rho^N(0), \widehat{\rho}^N(0)) &= \sum_{i=0}^{n-1} \int_{\bar{x}_i}^{\bar{x}_{i+1}^N} \Big(\alpha_i^N l_N - \rho_i^N(t)\,(x - \bar{x}_i) \Big)\, dx \\
&= \sum_{i=0}^{n-1} \alpha_i^N l_N \int_{\bar{x}_i}^{\bar{x}_{i+1}} \left(1 - \frac{x - \bar{x}_i}{\bar{x}_{i+1} - \bar{x}_i} \right) dx \\
&\leq \max_{i=0,\dots,n} \{\alpha_i^N\} l_N \,(\bar{x}_n - \bar{x}_0)
\end{aligned} \tag{36}$$

$\Rightarrow$ it suffices to prove that $(\widehat{\rho}^N(0))_{n\in\mathbb{N}}$ converges to $\bar{\rho}$ in sense of $\mathrm{W}_{L,1}$- distance

- Using expressions of both Euler (11) and empirical (30) discrete densities

$$\begin{aligned}
&\mathrm{W}_{L,1}(\widehat{\rho}^N(0), \bar{\rho}) \\
&= \sum_{i=0}^{n-2} \int_{\bar{x}_i}^{\bar{x}_{i+1}} \left(\left(\sum_{j=0}^{i-1} \alpha_j^N l_N - \int_{\bar{x}_0}^{\bar{x}_i} \bar{\rho}(y) dy \right) + \left(\alpha_i^N l_N - \int_{\bar{x}_i}^{x} \bar{\rho}(y) dy \right) \right) dx \\
&\qquad + \int_{\bar{x}_{n-1}}^{\bar{x}_n} \left(\sum_{j=0}^{n-2} \alpha_j^N l_N - \int_{\bar{x}_0}^{\bar{x}_{n-1}} \bar{\rho}(y) dy \right) + \left(\alpha_{n-1}^N l_N - \int_{\bar{x}_{n-1}}^{x} \bar{\rho}(y) dy \right) dx
\end{aligned}$$

Sketch of proof

- From atomization of initial density (31)

$$
\begin{aligned}
&\mathrm{W}_{L,1}(\widehat{\rho}^N(0), \bar{\rho}) \\
&\leq \sum_{i=0}^{n-2} \int_{\bar{x}_i}^{\bar{x}_{i+1}} \left(\alpha_i^N l_N - \int_{\bar{x}_i}^{x} \bar{\rho}(y)dy \right) dx + \int_{\bar{x}_{n-1}}^{\bar{x}_n} \left(\alpha_{n-1}^N l_N - \int_{\bar{x}_{n-1}}^{x} \bar{\rho}(y)dy \right) dx \\
&= \sum_{i=0}^{n-1} \alpha_i^N l_N \int_{\bar{x}_i}^{\bar{x}_{i+1}} \left(1 - \frac{1}{\alpha_i^N l_N} \int_{\bar{x}_i}^{x} \bar{\rho}(y)dy \right) dx \\
&\leq \max_{i=0,\dots,n} \left\{ \alpha_i^N \right\} l_N (\bar{x}_n - \bar{x}_0)
\end{aligned}
$$

Sketch of proof

- From atomization of initial density (31)

$$
\begin{aligned}
&\mathrm{W}_{L,1}(\widehat{\rho}^N(0), \bar{\rho}) \\
&\le \sum_{i=0}^{n-2} \int_{\bar{x}_i}^{\bar{x}_{i+1}} \left(\alpha_i^N I_N - \int_{\bar{x}_i}^{x} \bar{\rho}(y)dy \right) dx + \int_{\bar{x}_{n-1}}^{\bar{x}_n} \left(\alpha_{n-1}^N I_N - \int_{\bar{x}_{n-1}}^{x} \bar{\rho}(y)dy \right) dx \\
&= \sum_{i=0}^{n-1} \alpha_i^N I_N \int_{\bar{x}_i}^{\bar{x}_{i+1}} \left(1 - \frac{1}{\alpha_i^N I_N} \int_{\bar{x}_i}^{x} \bar{\rho}(y)dy \right) dx \\
&\le \max_{i=0,\dots,n} \left\{ \alpha_i^N \right\} I_N(\bar{x}_n - \bar{x}_0)
\end{aligned}
$$

- From (35)-(36), conclude that $(\rho^N(0))_{n\in\mathbb{N}}$ converges to $\bar{\rho}$ in sense of $\mathrm{W}_{L,1}$-Wasserstein distance

Sketch of proof

- From atomization of initial density (31)

$$
\begin{aligned}
&\mathrm{W}_{L,1}(\widehat{\rho}^N(0),\bar{\rho})\\
&\leq \sum_{i=0}^{n-2}\int_{\bar{x}_i}^{\bar{x}_{i+1}}\left(\alpha_i^N l_N-\int_{\bar{x}_i}^{x}\bar{\rho}(y)dy\right)dx+\int_{\bar{x}_{n-1}}^{\bar{x}_n}\left(\alpha_{n-1}^N l_N-\int_{\bar{x}_{n-1}}^{x}\bar{\rho}(y)dy\right)dx\\
&=\sum_{i=0}^{n-1}\alpha_i^N l_N\int_{\bar{x}_i}^{\bar{x}_{i+1}}\left(1-\frac{1}{\alpha_i^N l_N}\int_{\bar{x}_i}^{x}\bar{\rho}(y)dy\right)dx\\
&\leq \max_{i=0,\dots,n}\left\{\alpha_i^N\right\} l_N(\bar{x}_n-\bar{x}_0)
\end{aligned}
$$

- From (35)-(36), conclude that $(\rho^N(0))_{n\in\mathbb{N}}$ converges to $\bar{\rho}$ in sense of $\mathrm{W}_{L,1}$-Wasserstein distance
- Finally generalize convergence to unique entropy solution of conservation law (6)
  $\Rightarrow$ require only minor modifications to arguments in **francesco˙rigorous˙2015**